

## INVESTIGATING THE NANOSTRUCTURAL EVOLUTION OF TiO<sub>2</sub> NANOPARTICLES IN THE SOL-GEL DERIVED TiO<sub>2</sub>-POLYMETHYL METHACRYLATE NANOCOMPOSITES

Akhmad Herman Yuwono<sup>1\*</sup>, Yu Zhang<sup>2</sup>, John Wang<sup>2</sup>

<sup>1</sup>*Department of Metallurgy and Materials Engineering, Faculty of Engineering  
Universitas Indonesia, Depok 16424, Indonesia*

<sup>2</sup>*Department of Materials Science and Engineering, Faculty of Engineering  
National University of Singapore, Singapore 117574*

(Received: May 2010 / Revised: June 2010 / Accepted: July 2010)

### ABSTRACT

Nanocomposite thin films consisting of titanium oxide, or TiO<sub>2</sub>, nanoparticles embedded in a polymer matrix represent a new class of potential materials for optoelectronic applications such as optical switches, waveguides, high refractive indices and non-linear optical devices. Among the various processing techniques under development for these nanocomposites, the *in situ* sol-gel process is known to be versatile as it enables control of the inorganic-organic interaction at various molecular, nanometer, and micrometer scales. However, the sol-gel process has a major limitation, which is the low crystallinity in the resulting TiO<sub>2</sub> phase due to relatively low processing temperatures. Therefore, the current research is aimed at investigating the nanostructural evolution of the TiO<sub>2</sub> crystallite during the *in situ* sol-gel process to gain a better understanding of the mechanisms responsible for the largely amorphous nature of TiO<sub>2</sub> nanoparticles. For this purpose, two sol-gel parameters, i.e., the hydrolysis ratio ( $R_w$ ) and pH value of the TiO<sub>2</sub> precursor solution were varied. On the basis of XRD and FTIR analyses, it was found that the largely amorphous TiO<sub>2</sub> state is related to the fast development of stiff Ti-OH networks during the hydrolysis and condensation stages of the sol-gel process, and concurrently worsened by the formation of the rigid PMMA matrix upon thermal annealing.

*Keywords:* Hydrolysis ratio; Inorganic-organic nanocomposites; pH; TiO<sub>2</sub> nanostructural evolution

### 1. INTRODUCTION

An incorporation of titanium dioxide (TiO<sub>2</sub>) nanoparticles into poly(methyl methacrylate) or PMMA through *in situ* sol-gel polymerization technique has been well-known for preparing high-refractive index coating for optoelectronic applications. Zhang et al. (1997) synthesized TiO<sub>2</sub>-PMMA nanocomposites using chelating ligand as a coupling agent, followed Chen et al. (1999, 2001) who synthesized thin film TiO<sub>2</sub>-PMMA nanocomposites by the *in situ* sol-gel process of trialkoxysilane-capped PMMA-titania combined with spin coating and a multi-step annealing process. It has been shown also in our previous works (Yuwono, 2003; Elim, 2003) that this nanocomposite can exhibit a very fast recovery time of ~1.5 picoseconds and a large third order nonlinear optical susceptibility,  $\chi^{(3)}$ , which benefit for optoelectronic

---

\* Corresponding author's email: [ahyuwono@metal.ui.ac.id](mailto:ahyuwono@metal.ui.ac.id), Tel. +62-21-7863510, Fax. +62-21-7872350

devices such as nonlinear optical switching devices in photonics and real-time coherent optical signal processors (Wang et al., 1991; Fischer et al., 1995). However, it is realized that TiO<sub>2</sub>-PMMA nanocomposites are limited by the occurrence of amorphous TiO<sub>2</sub> nanoparticles, which cannot be avoided under the conditions tolerable by the polymer matrix during the low temperature sol-gel process. Therefore, it is our main interest to investigate the factors causing the amorphous nature of the TiO<sub>2</sub> phase in the PMMA matrix. For this purpose, several synthesis parameters involved in the *in situ* sol-gel polymerization, including the pH value, water content, or hydrolysis ratio ( $R_w$ ), and coupling agent concentration of the TiO<sub>2</sub> precursor solution were systematically investigated in the current work.

## 2. EXPERIMENTAL

An *in-situ* sol-gel polymerization process was carried out for preparing TiO<sub>2</sub>-PMMA nanocomposites in this work. This technique is basically a thorough mixing process between a pre-hydrolyzed TiO<sub>2</sub> precursor (titanium isopropoxide, Ti-iP) and pre-polymerized PMMA. First, the monomers, methyl methacrylate (MMA, 99%, Acros) and coupling agent 3-(trimethoxysilyl)propyl methacrylate (MSMA, 98%, Acros), and initiator benzoyl peroxide (BPO, 98%, Acros) in solvent tetrahydrofuran (THF, 99%, Acros) were added into a reaction flask and polymerized at 60°C for 1 hour. The molar ratio of MSMA to MMA+ MSMA (coupling agent concentration) was controlled at 0.25 and the amount of BPO added to the mixture was fixed at 3.75 mol%. Furthermore, a TiO<sub>2</sub> based sol solution was prepared by mixing titanium isopropoxide (Ti-iP, 98%, Acros) with ethyl alcohol (Et-OH, 95%, Merck) in a container and stirred for 30 minutes. A mixture of de-ionized water and hydrochloric acid (HCL, 36%, Ajax) was then added under stirring condition into the transparent solution to promote hydrolysis. The Ti-iP concentration in the solution was controlled at 0.4 M.

For investigation purposes, three different sols with different pH values of 3.08, 1.08 and 0.33 were firstly prepared under the same ratio of water to Ti-iP ( $R_w$ ), or a hydrolysis ratio of 0.82. At the same time, other sols with various hydrolysis ratios of 0.82, 2.00 and 3.50 under the same pH value of 0.78 were also synthesized. For another variation, in addition to the above mentioned coupling agent concentration of 0.25, the amount of MSMA/(MSMA+MMA) molar ratio was reduced to 0.05 and the resulting nanocomposite was compared to that derived from 0.25. All of these parameters were thoroughly varied while maintaining the stability of sol solutions to be clear and transparent. Finally, this transparent sol solution was carefully added dropwise over a duration of 30 minutes into the partially polymerized monomers (MMA and MSMA) with rigorous stirring to avoid local inhomogeneities. The reaction was allowed to proceed at 60°C for another 2 hours. In this study, the weight ratio (%wt) between the inorganic and organic precursors in the reaction mixture was fixed consistently at 60:40. The thin film was fabricated by spin coating the hybrid solution onto glass substrates at 3000 rpm for 20 seconds. The coated films were then annealed at 60°C for 30 minutes and 150°C for 3 hours. The nanocomposites characterization was carried out with X-ray diffraction (XRD) measurements on a Bruker AXS  $\theta$ -2 $\theta$  diffractometer using Cu K- $\alpha$  radiation (1.5406 Å) and Fourier Transform Infrared (FTIR) spectroscopy in the range of 4000-400 cm<sup>-1</sup> using the Bio-Rad model QS-300 spectrometer.

## 3. RESULTS AND DISCUSSION

### 3.1. Effect of pH value

Brinker and Hurd (1994) and Langlet et al. (2001) proposed that the amorphous state of TiO<sub>2</sub> was caused by the formation of stiff Ti-OH arising from fast condensation. Yoldas (1979) also suggested that if the rate of condensation process is faster than hydrolysis, the alkyl groups are incorporated into the structure and sterically hinder the formation of ordered structure.

Therefore, in order to enable the precursor to crystallize into an equilibrium structure, the condensation process should proceed slowly after the completion of hydrolysis. Lowering the pH value of the titania solution has been considered effective in enhancing the rate of hydrolysis and inhibiting condensation (Livage et al., 1988). Consequently, this promotes the hydrolysis process and at the same time decreases the rate of condensation significantly since the protonated species reduce their interaction by repelling each other. Yoldas (1986) and Kallala et al. (1992) have shown that a difference in the inhibition ratios can lead to formation of sols, transparent gels, turbid gels or precipitates. Accordingly, Gopal et al. (1997) and Watson et al. (2004) have reported the formation of anatase and rutile  $\text{TiO}_2$  synthesized directly from an acid-catalyzed solution at temperatures close to room temperature. For the nanocomposites investigated in this study, however, a question remains as to whether a slow condensation rate of the protonated titanium hydroxide can lead to the densification of  $\text{TiO}_2$  during the subsequent annealing process, while at the same time polymerization of the MMA monomers takes place effectively. The latter is responsible for the fast trapping effect causing a largely amorphous  $\text{TiO}_2$  phase in the polymer matrix. Therefore, it will be of further interest to investigate the effect of pH value on the nanocrystallinity of  $\text{TiO}_2$  phase in nanocomposites. For the investigation,  $\text{TiO}_2$ -PMMA nanocomposites were derived from  $\text{TiO}_2$  sol solutions of pH value varying in the range of 3.08 to 0.33. This was done by adjusting the amount of hydrochloric acid (HCl) added, the function of which is to control the hydrolysis and condensation rates of titanium alkoxide (Kallala et al., 1992; Burgos et al., 1999). The water to titanium alkoxide ratio ( $R_w$ ) in each solution was kept at 0.82. Prior to mixing with the organic constituent, the sols were stirred at room temperature for 72 hours, aimed at providing sufficient time for the protonation of titanium alkoxide to take place, in accordance with the amount of hydrochloric acid added into the sol precursors. The XRD traces of the thus derived nanocomposites are shown in Figure 1. It is noted that the nanocomposite derived from the inorganic sol solution of pH 3.08 (trace “(a)”) is highly amorphous as indicated by the occurrence of two broadened humps in the  $2\theta$  ranges of  $20\text{-}35^\circ$  and  $40\text{-}55^\circ$ . By contrast, diffraction peaks at  $2\theta$  of  $\sim 25$  and  $48^\circ$  corresponding to (101) and (200) crystal planes of anatase  $\text{TiO}_2$  were observed for the nanocomposites derived from the inorganic sol solution of pH 1.08 and 0.33 (traces “(b)” and “(c)”).

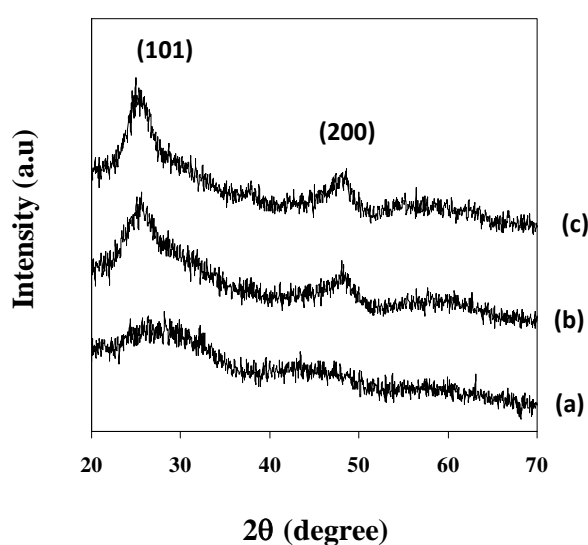


Figure 1 XRD traces of the nanocomposite derived from inorganic sol solution with pH values of (a) 3.08, (b) 1.08, and (c) 0.33, respectively

The results can be interpreted by considering the role of  $\text{H}^+$  ion in providing repulsion forces

among the protonated inorganic species. It is known that a highly acidic protonation leads to a stronger repulsion force and thus formation of extended structure from the hydrolyzed alkoxide (Chiang et al. 2003). By using small-angle X-ray scattering (SAXS), Xiong et al. (2004, 2005) investigated the structure of inorganic species in trialkoxysilane-capped acrylic-titania hybrids derived from titania sols under three typical pH values of 4.4, 7.0 and 8.8, representing acid, neutral, and basic conditions, respectively. They observed that under the basic condition the inorganic domains can reach a radius of gyration ( $R_g$ ) and fractal dimension ( $D$ ) of 7.3 nm and 1.35. However, under the acid condition, the values were only 2.4 nm and 0.18, respectively. The smaller sizes in the latter were associated with the restriction of inorganic chain-like structures into open regions of the mesh produced by the cross-linked polymers (Xiong et al., 2004, 2005). On the other hand, the notable diffraction peaks in the XRD traces “(b)” and “(c)” for the nanocomposites derived from TiO<sub>2</sub> sols with a much lower pH value (1.08 and 0.33) suggest a rather different mechanism in comparison to what has been proposed by Xiong et al. (2004, 2005) for the acid catalyst condition. In the system investigated in this work, the linear chain-like structures of hydrolyzed inorganic precursors were able to perform further self-densification in the solution stage. It proceeded up to the stage when the nanocomposite sample was annealed, whereby a rigid organic PMMA network was formed. The nanocrystallinity of the sample derived from the sol solution with a much lower pH value, *i.e.*, 0.33 (trace “(c)”) is slightly higher than that of 1.08 (trace “(b)”). It suggests that the stronger repulsion force created among the protonated species at lower pH values can induce a better densification for TiO<sub>2</sub> phase in the TiO<sub>2</sub>-PMMA nanocomposite system.

### 3.2. Effect of water to alkoxide ratio

The water to alkoxide ( $R_w$ ) determines the potential functionality of inorganic monomers in building the network (Kallala et al., 1993). In the previous investigation, an  $R_w$  of 0.82 was consistently used for the TiO<sub>2</sub> sol, which is stable and does not turn into a gel prior to mixing with a polymer matrix. However, this ratio is less than the required stoichiometric value, *i.e.*, 4.00. As a result, the alkoxide precursor experienced an incomplete hydrolysis process. It is therefore of interest to find out whether the amount of water during sol preparation can favor a more complete hydrolysis and thus provide a higher nanocrystallinity for the titania phase in nanocomposite. For investigation, three different sols with  $R_w$  of 0.82, 2.00 and 3.50 under the same pH value of 0.78 were prepared. All the TiO<sub>2</sub> sol solutions were transparent and stable. An attempt to increase  $R_w$  to 4.00 led to the immediate formation of a gel which could not be incorporated homogeneously into pre-polymerized PMMA. Therefore, the first three compositions were used for further investigations. The XRD traces of the resulting nanocomposites are given in Figure 2.

It is shown that when  $R_w$  is 0.82, the resulting nanocomposite (trace “(a)”) demonstrates two broadened diffraction peaks at  $2\theta$  of  $\sim 25.35^\circ$  and  $48.12^\circ$  corresponding to (101) and (200) crystal planes of the anatase TiO<sub>2</sub> phase. An increase in  $R_w$  to 2.00 did not lead to a significant enhancement in nanocrystallinity for the respective nanocomposite (trace “(b)”). However, there was an onset of additional two peaks at  $2\theta$  of  $38.63^\circ$  and  $55.08^\circ$  corresponding to (112) and (211) crystal planes. Further increase of  $R_w$  to 3.50 gave rise to the unexpected occurrence of an amorphous TiO<sub>2</sub> phase. The above observation can be analyzed by considering that an increase in  $R_w$  gives rise to a stronger nucleophilic reaction between water and alkoxide species, and thus more -OR groups bonded to metal were substituted by -OH network structures. A larger and more compact structure of inorganic domains, as a result of the formation of a three-dimensional network structure, is therefore expected with the completion of the -OH network (Xiong et al., 2004, 2005).

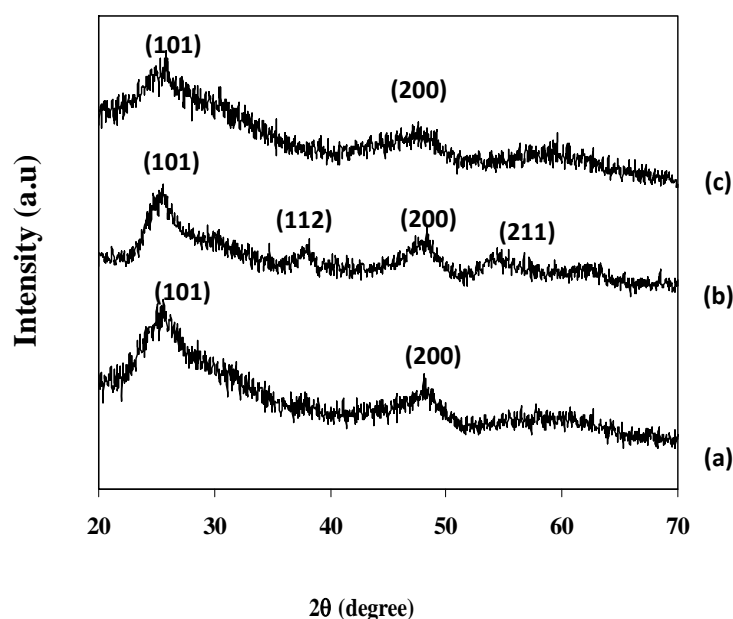


Figure 2 XRD traces of the nanocomposite derived from inorganic sol solution with  $R_w$  of (a) 0.82, (b) 2.00, and (c) 3.50, respectively

Based on the XRD results, however, such increase in the inorganic domain size to form bigger nanocrystallites was not clearly indicated when  $R_w$  was increased from 0.82 to 2.00, as shown by the diffraction peaks' intensity at  $2\theta$  of  $\sim 25.35^\circ$  and  $48.12^\circ$ . Yu et al. (2000) described a transition model of the inorganic domains in  $\text{TiO}_2$ - $\text{SiO}_2$  nanocomposite whereby chain-like structures transformed into particle-like clusters when  $R_w$  was varied from a value below the stoichiometric ratio ( $<4.00$ ) to that of above the critical value ( $>4.00$ ). The appearance of two additional peaks at  $2\theta$  of  $38.63^\circ$  and  $55.08^\circ$  suggested that the high number of  $-\text{OH}$  groups generated at  $R_w$  of 2.00 had provided more  $\text{TiO}_2$  nuclei which further grew as nanocrystallites of different directions in addition to what had been formed at  $R_w$  of 0.82. It is of interest to compare the current result with a previous work performed by Xiong et al. (2004) who employed the SAXS technique to investigate the effect of water content on the structures of thermoplastic acrylic resin-titania hybrids. They observed that nanocomposites derived from  $R_w$  of 1.00 and 2.00 demonstrated shallow linear regions in the Guinier and Porod plots, indicating little phase separation. Besides, the difference in scattering intensity between hybrids derived from  $R_w$  of 1.00 and 2.00 was small. This condition is very similar to the nanocomposites with  $R_w$  of 0.82 and 2.00 in the present study, as revealed by XRD results in Figure 2. However, at high  $R_w$ , a discrepancy occurs between the current result and what has been observed by Xiong et al. (2004). In their study, further increase of  $R_w$  up to 4.00 led to a denser inorganic phase with a larger size. In contrast, the nanocomposite derived from the hydrolysis ratio,  $R_w$  of 3.50, is highly amorphous when compared with those derived from 0.82 and 2.00. Again, this condition is associated with the trapping of the hydrolyzed alkoxide groups by the rigid PMMA network during and after annealing at  $150^\circ\text{C}$ . It is highly possible that although a great number of  $-\text{OH}$  groups were generated through the relatively complete hydrolysis due to the strong constraint effect by the organic polymer matrix, they failed to proceed to the subsequent densification. Hence, the nanocrystalline  $\text{TiO}_2$  phase was not achieved. In connection with the discrepancy observed between the two studies, it should be noted that Xiong et al. (2004a, 2004b, 2005) relied on the SAXS scattering patterns in order to determine the sizes of inorganic phases in the hybrid composition. Indeed, several variations in their synthesis process such as pH value, water content and solvent mixture which led to

different levels of hydrolysis and condensation for titania precursor could result in different levels of phase separation and thus scattering patterns accordingly. It was not confirmed whether the inorganic network formed in the hybrids represented amorphous Ti-OH, nanocrystalline TiO<sub>2</sub> or a mixture of both. Therefore, the observed scattering pattern can be considered as a response from the cumulative quantity of inorganic phases, regardless of their amorphous or crystalline nature. As a result, the SAXS studies of Xiong et al. (2004a, 2004b, 2005) were not affected by the trapping mechanism of the TiO<sub>2</sub> phase by the polymer matrix, as encountered in the nanocomposites investigated in the current study.

### 3.3. Effect of coupling agent concentration

In the present study, 3-(trimethoxysilyl)propyl methacrylate (MSMA) is introduced as a coupling agent between the inorganic titanium alkoxide precursor and the organic MMA matrix. In our previous work (Yuwono 2003; Elim 2003) a constant MSMA/(MSMA+MMA) molar ratio of 0.25 was used in the nanocomposite preparation. Thermal gravimetric analysis (TGA) and FTIR studies confirmed that the thus derived nanocomposites demonstrated a strong interaction between the inorganic and organic moieties. For optical properties, this can be beneficial since the resulting nanocomposite is transparent in the visible region. On the other hand, such a strong bonding may have a reverse effect on the TiO<sub>2</sub> formation, *i.e.*, the strong hindrance experienced by the hydrolyzed titanium alkoxide (Ti-OH networks) in PMMA gave rise to a largely amorphous TiO<sub>2</sub> phase. Therefore it is of further interest to investigate whether an incorporation of a lower concentration of the coupling agent at the solution preparation stage can provide a higher flexibility for the hydrolyzed titanium alkoxide to undergo densification in the PMMA matrix during the subsequent annealing process. By doing so, it is expected that Ti-O-Ti bonds will be able to develop a long-range order, such that nanocrystalline TiO<sub>2</sub> particles can be formed. The amount of MSMA/(MSMA+MMA) molar ratio was reduced to 0.05 and the resulting nanocomposite was compared to that derived from 0.25 Figure 3 presents the XRD traces for both nanocomposites showing two broadened phase peaks at  $2\theta$  angles of 25.35 and 48.12° that can be assigned to (101) and (200) crystal planes of the anatase phase. The nanocomposite derived from the coupling agent ratio of 0.05 shows slightly stronger diffraction peaks than those derived from the coupling agent ratio of 0.25.

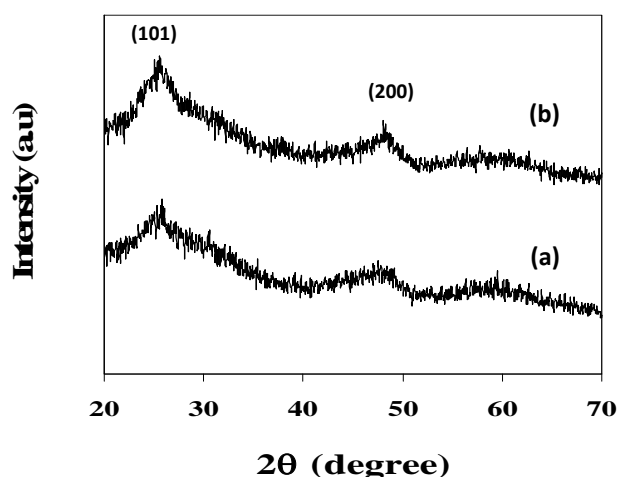


Figure 3 XRD traces of nanocomposite derived from ratio MSMA/(MSMA+MMA) ratio of (a) 0.25 and (b) 0.05

For further confirmation, FTIR spectroscopy of the two nanocomposites was investigated. The stretching vibrations for both samples are shown in Figures 4a and 4b, for both low

wavenumber range ( $1100\text{--}400\text{ cm}^{-1}$ ) and high wavenumber range ( $4000\text{--}2400\text{ cm}^{-1}$ ), respectively. Figure 4a shows the occurrence of absorption bands located at  $450$  and  $650\text{ cm}^{-1}$  which can be assigned to Ti–O and Ti–O–Ti stretching vibrations, respectively, as the characteristic of nanocrystalline  $\text{TiO}_2$  in short and long range order (Djaoed et al., 2002; Wang et al., 1999). In addition, there is an additional band at  $910\text{ cm}^{-1}$ , corresponding to the stretching vibration of Ti–O–Si bond (Leaustic et al., 1989). Although the two nanocomposites show similar intensities, however, a careful comparison reveals that a considerably higher band intensity occurs in the range of  $1000\text{--}1200\text{ cm}^{-1}$  in spectrum "(ii)", in comparison to spectrum "(i)". This band, with the strongest absorption peak located at  $\sim 1080\text{ cm}^{-1}$ , is assigned to the Ti–O–C stretching mode originating from the remaining unhydrolyzed alkoxy groups (Que et al., 2000; Zhang et al., 2001). Although there is a possibility of overlapping with C–O–C bonds originating from the PMMA matrix in the range of  $1039\text{--}1192\text{ cm}^{-1}$  (Chen et al., 1999), the same amount of MMA monomer was incorporated into both nanocomposites. This was further confirmed by checking the stretching vibration of C–H bond at  $2950\text{ cm}^{-1}$  as shown in Fig. 4b. Both spectra "(i)" and "(ii)" are very similar in intensity. Therefore it can be concluded that the enhanced intensity at  $\sim 1080\text{ cm}^{-1}$  in spectrum "(ii)" of Fig. 4a is related to the higher number of Ti–O–C bonds in the nanocomposite derived from the lower coupling agent ratio.

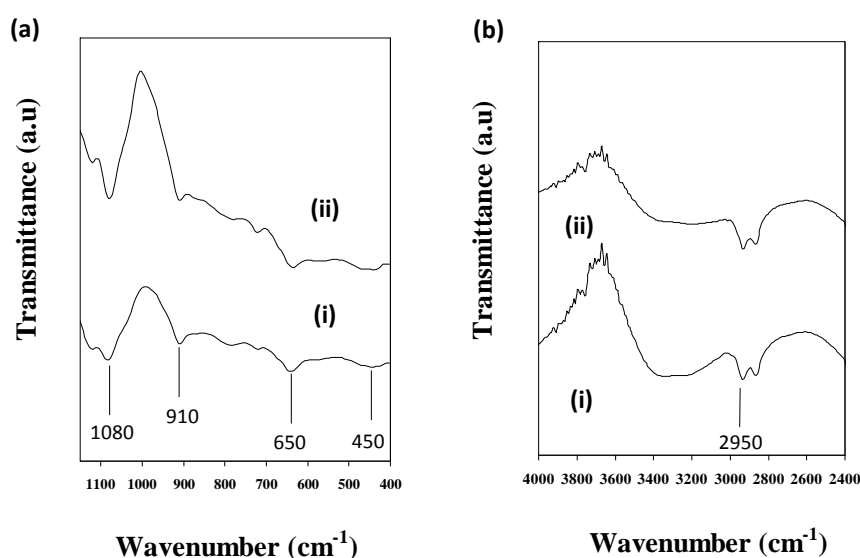


Figure 4 FTIR spectra of  $\text{TiO}_2$ –PMMA nanocomposites derived from MSMA/ (MSMA+MMA) ratio of (i) 0.25 and (ii) 0.05 in the: (a) low wavenumber range of  $1100\text{--}400\text{ cm}^{-1}$ , and (b) high wavenumber range of  $4000\text{--}2400\text{ cm}^{-1}$

It is of further interest to investigate the reason behind the enhanced nanocrystallinity shown by the nanocomposite derived from the lower coupling agent ratio. One approach is observe the three absorption bands; Ti–OH at  $\sim 3400\text{ cm}^{-1}$ , Ti–O–C at  $1080\text{ cm}^{-1}$ , and Ti–O–Si at  $910\text{ cm}^{-1}$ . As seen in Fig. 4b, the intensity of the Ti–OH band for the nanocomposite derived from the coupling agent ratio of 0.05 (spectra "(ii)") is lower than that derived from 0.25 (spectra "(i)"), while a higher intensity of the Ti–O–C band (Fig. 4a) is demonstrated by the former. In contrast to these differences, both nanocomposite show more or less the same intensity for the Ti–O–Si band at  $910\text{ cm}^{-1}$ . As suggested by Brinker and Hurd (1999) and Langlet et al. (2001), the largely amorphous  $\text{TiO}_2$  thin films obtained at low temperatures are due to the formation of stiff Ti–OH networks resulting from the fast condensation of titanium alkoxide precursor, which in turn hinder the densification of crystallite  $\text{TiO}_2$  phase. In this connection, therefore, the low intensity of Ti–OH observed for the nanocomposite derived from the lower coupling agent ratio

suggests a reduced amount of amorphous phase. On the other hand, the high intensity of the Ti–O–C stretching mode from the unhydrolyzed alkoxy groups in this sample is related to the high number of interfacial sites for TiO<sub>2</sub> nucleation. The interfacial bond is not as stiff as the Ti–OH network and is therefore sufficiently flexible to take part in the densification of the TiO<sub>2</sub> phase, *i.e.*, by the arrangement of Ti–O–Ti bonds in the long-range order. Thus, an enhancement in TiO<sub>2</sub> nanocrystallinity resulted, as detected by XRD (Fig. 3). Zhang et al. (2001) has reported that the Ti–O–C bond, together with Ti–O and Ti–OH, can lead to connected networks of TiO<sub>2</sub> nanoparticles in titania-poly(phenylenevinylene) or TiO<sub>2</sub>-PPV nanocomposites. The interfacial phase plays an important role in providing the necessary dispersion function and thus preventing the agglomeration of TiO<sub>2</sub> nanoparticles in the polyvinyl alcohol (PVA) matrix (Chen et al., 2002).

#### 4. CONCLUSION

In an attempt to understand the mechanism responsible for the largely amorphous nature of the TiO<sub>2</sub> phase in the nanocomposites, several processing parameters involved in sol-gel and *in situ* polymerization were investigated, including coupling agent concentration, pH value, and water to alkoxide ratio. Variations of pH value and water to alkoxide ratios in the TiO<sub>2</sub> sol solution did not effectively lead to a significant enhancement in the nanocrystallinity of the TiO<sub>2</sub> phase in the resulting nanocomposites. On the basis of XRD and FTIR analyses, the mechanism behind the amorphous nature of the TiO<sub>2</sub> phase in TiO<sub>2</sub>-PMMA nanocomposites is better understood. It is due to the fast development of stiff Ti–OH networks during hydrolysis and condensation, which occurs concurrently with the rigid entrapment, resulting from the polymerization of organic the PMMA matrix during thermal annealing process. The nanocrystallinity enhancements are shown to be more pronounced in the nanocomposite derived from a lower coupling agent ratio of 0.05, as a consequence of a more loosely linked interfacial bonding between inorganic and organic segments, in comparison to the nanocomposite derived from a higher coupling agent ratio of 0.25.

#### 5. REFERENCES

- Brinker, C.J. & Hurd, A.J., 1994. Fundamentals of sol-gel dip-coating, *J. Phys. III France* Volume 4, pp.1231-1242.
- Burgos, M. & Langlet, M., 1999. The sol-gel transformation of TIPT coatings: a FTIR study, *Thin Solid Films*, Volume 349, pp.19-23.
- Chen, W. C., Lee, S. J., Lee, L.H. & Lin, J. L., 1999. Synthesis and characterization of trialkoxysilane capped poly(methylmethacrylate) – titania hybrid optical thin film, *J. Mater. Chem.*, Volume 9, pp. 2999-3003.
- Chen, X.C., 2002. Preparation and property of TiO<sub>2</sub> nanoparticle dispersed polyvinyl alcohol composite materials, *J. Mater. Sci. Lett.* Volume 21, pp.1637-1639.
- Chiang, C.L., Ma, C.C., Wu, D. L. & Kuan, H.C., 2003. Preparation, characterization, and properties of novolac-type phenolic/SiO<sub>2</sub> hybrid organic-inorganic nanocomposite materials by sol-gel method, *J. Polym. Sci. Polym. Chem.*, Volume 41, pp.905-913.
- Djaoued, Y., Badilescu, S., Ashrit, P.V., Bersani, D., Lottici, P.P. & Brüning, R., 2002. Low Temperature Sol-Gel Preparation of Nanocrystalline TiO<sub>2</sub> Thin Films, *J. of Sol-Gel. Sci. Technol.*, Volume 24, pp.247-254.
- Elim, H.I., Ji, W., Yuwono, A.H., Xue, J.M. & Wang, J., 2003. Ultrafast optical nonlinearity in poly(methylmethacrylate)-TiO<sub>2</sub> nanocomposites, *Appl. Phys. Lett.*, Volume 82 Number 16, pp.2691-2693.
- Fischer, G.L., Boyd, R.W., Gehr, R.J., Jenekhe, S.A., Osaheni, J.A., Sipe J.E. & Weller-Brophy, L.A., 1995. Enhanced nonlinear optical response of composite materials *Phys. Rev. Lett.*, Volume 74, Number 10, pp.1871-1874.

- Gopal, M., Moberly Chan, W.J. & De Jonghe, L.C., 1997. Room temperature synthesis of crystalline metal oxides, *J. Mater. Sci.*, Volume 32, pp.6001-6008.
- Kallala, M., Sanchez, C. & Cabane, B., 1992. SAXS study of gelation and precipitation in titanium-based systems, *J. Non-Crys.Solids*, Volume 147-148, pp.189-193.
- Kallala, M., Sanchez, C. & Cabane, B., 1993. Structures of inorganic polymers in sol-gel processes based on titanium oxide, *Phys. Rev. E*, Volume 48, pp.3692-3704.
- Langlet, M., Burgos, M., Couthier, C., Jimenez, C., Morant, C. & Manso, M., 2001. Low Temperature Preparation of High Refractive Index and Mechanically Resistant Sol-gel TiO<sub>2</sub> Films for Multilayer Antireflective Coating Applications, *J. Sol-Gel. Sci. Technol.*, Volume 22, pp.139-150.
- Leaustic, A., Babonneau, F. & Livage, J., 1989. Structural investigation of the hydrolysis-condensation process of titanium alkoxides Ti(OR)<sub>4</sub> (OR = OPr-iso, OEt) modified by acetylacetone. 1. Study of the alkoxide modification, *Chem. Mater.* Volume 1, pp.240-247.
- Lee, L. H. & Chen, W.C., 2001. High-Refractive-Index Thin Films Prepared from Trialkoxysilane-Capped Poly(methyl methacrylate)-Titania Materials, *Chem. Mater.*, Volume 13, pp.1137-1142.
- Livage, J., Henry, M. & Sanchez, C., 1988. Sol-gel chemistry of transition metal oxides, *Prog. Solid State Chem.*, Volume 18, pp.259-341.
- Que, W., Zhou, Y., Lam, Y.L., Chan, Y.C., Cheng, S.D., Sun Z. & Kam, C.H., 2000. Microstructural and Spectroscopic Studies of Sol-Gel Derived Silica-Titania Waveguide, *J. Sol-Gel. Sci. Technol.*, Volume 18, pp.77-83.
- Wang, B., Wilkes, G.L., Hedrick, J.C., Liptak, S.C. & McGrath, J.E., 1991. New high-refractive-index organic/inorganic hybrid materials from sol-gel processing Macromolecules, Volume 24, pp.3449-3450.
- Wang, S.X., Wang, M.T., Lei, Y. & Zhang, L.D., 1999. "Anchor effect" in poly(styrene maleic anhydride)/TiO<sub>2</sub> nanocomposites, *J. Mater. Sci. Lett.*, Volume 18, pp.2009-2012.
- Watson, S., Beydoun, D., Scott, J. & Amal, R., 2004. Preparation of nanosized crystalline TiO<sub>2</sub> particles at low temperature for photocatalysis, *J. Nanopart. Res.*, Volume 6, pp.193-207.
- Xiong, M., Zhou, S., Wu, L., Wang B. & Yang, L., 2004. Sol-gel derived organic-inorganic hybrid from trialkoxysilane-capped acrylic resin and titania: effects of preparation conditions on the structure and properties, *Polymer*, Volume 45, pp.8127-8138.
- Xiong, M., Zhou, S., You, B. & Wu, L., 2005. Trialkoxysilane-capped acrylic resin/titania organic-inorganic hybrid optical films prepared by the sol-gel process, *Polymer*, Volume 43, pp.637-649.
- Xiong, M.N., Zhou, S.X., You, B., Gu, G.X. & Wu, L.M., 2004. Effect of preparation of titania sol on the structure and properties of acrylic resin/titania hybrid materials, *J. Polym. Sci. Polym. Phys.*, Volume 42, pp.3682-3694.
- Yoldas, B.E., 1979. Formation of titania-silica glasses by low temperature chemical polymerization, *J. Mater. Sci.*, Volume 14, pp.1843-1849.
- Yoldas, B.E., 1986. Zirconium oxides formed by hydrolytic condensation of alkoxides and parameters that affect their morphology, *J. Mater. Sci.*, Volume 21, pp.1080-1086.
- Yu, H. F. & Wang, S.M., 2000. Effects of water content and pH on gel-derived TiO<sub>2</sub>-SiO<sub>2</sub> *J. Non-Cryst. Solids*, Volume 261, pp. 260-267.
- Yuwono, A.H., Xue, J.M., Wang, J., Elim, H.I., Ji, W., Li, Y. & White, T.J., 2003. White, Transparent nanohybrids of nanocrystalline TiO<sub>2</sub> in PMMA with unique nonlinear optical behavior, *J. Mater. Chem*, Volume 13, pp.1475-1479.
- Zhang, J., Ju, X., Wang, B.J., Li, Q.S., Liu T. & Hu, T.D., 2001. *Study on the optical properties of PPV/TiO<sub>2</sub> nanocomposites.*, *Synth. Met.* Volume 118, pp.181-185.
- Zhang, J., Luo, S. & Gui, L., 1997. Poly(methylmethacrylate)-titania hybrid materials by sol-gel processing, *J. Mater. Sci.*, Volume 32, pp.1469-1472.